IET Microwaves, Antennas & Propagation

Research Article

IET Journals
The Institution of Engineering and Technology

Compact 3D-loop antenna with bandwidth enhancement for WWAN/LTE mobile-phones applications

ISSN 1751-8725
Received on 23rd March 2016
Revised on 6th August 2016
Accepted on 31st August 2016
doi: 10.1049/iet-map.2016.0243
www.ietdl.org

Di Wu ✉, *Sing Wai Cheung*, *Tung Ip Yuk*

Department of Electrical and Electronic Engineering, The University of Hong Kong, Hong Kong, People's Republic of China
✉ *E-mail: diwu@eee.hku.hk*

Abstract: This study presents a 3D-loop antenna for wireless-wide-area network/long-term evolution (WWAN/LTE) operation. The size is compact and low profile and so the antenna is suitable for mobile-phone applications. The loop itself generates four resonant modes. Three parasitic elements are placed closely to the 3D-meandered loop radiator to generate three more resonant modes. These resonant modes form a dual-band, a lower band and a wide upper band, to cover many current mobile standards. The antenna performance, in terms of impedance bandwidth, efficiency, peak gain and radiation pattern, is studied using simulation. The antenna is also fabricated and the prototyped antenna is measured using the Satimo StarLab system. The measured results of the antenna inside a phone case on a phantom hand and phantom head in the data mode and talk mode, respectively, (defined by the Cellular Telephone Industries Association) are also presented. The measured efficiencies are subsequently used to estimate the total-radiated powers (TRPs). Results show that the TRPs in all covered standards meet the strictest over-the-air testing requirement of Vodafone.

1 Introduction

With the rapid development of cellular mobile communications standards, multi-band operation for mobile phones becomes a common feature. Mobile-phone antennas are generally required to support many frequency bands for the long-term evolution/wireless-wide-area network (LTE/WWAN) operation. At the same time, mobile-phone antennas are also required to be compact and low profile. To fulfil these requirements, different promising antennas for smartphones applications have been proposed such as the planar inverted-F antennas (PIFAs) in [1–3], the monopole antennas in [4–6], the frequency reconfigurable antennas in [7–9] and the loop antennas in [10–14]. PIFAs and monopole antennas usually require large clearances on the motherboards for better impedance bandwidths. For example, in [2–6], a large clearance of 15 mm was required. Frequency reconfigurable antennas could be very compact. In [7–9], the clearances required were only 5 mm. However, the RF front-end circuits required were quite complicated, making the technique less attractive.

Loop antennas can be low profile and require small clearances, hence they are a potential candidate for current mobile-phones applications. In the past decade, much effort has been spent to enhance the bandwidths of loop antennas for mobile phone applications in order to support more mobile standards [10–13]. However, most of those loop antennas could only generate three resonant modes [10–12] and only the design in [13] employing a 3D-meandered loop could generate the fourth resonant mode, but explanation on the generation mechanism was not given. The bandwidth of the loop antenna for the upper band was 1.71–2.17 GHz (0.46 GHz, 24%), which could not cover the new 4G-LTE standard such as LTE 2300, LTE2500 and LTE3500. Recently in [14], the authors proposed a 3D-meandered loop antenna which could also generate the fourth resonant. The antenna had a wider upper bandwidth of 0.88 GHz (41%), from 1.7 to 2.58 GHz but it still could not cover the important frequency bands of LTE2500 (2500–2690 MHz) for current 4G-LTE standard and LTE 3500 (3400–3600 MHz) for future 5G standard [15]. Thus bandwidth enhancement for loop antennas to cover the current 4G and future 5G standards is needed.

Parasitic-element loading is an effective technique to improve the impedance bandwidths of PIFAs [16] and monopoles [5, 6]. In this paper, it is proposed to use parasitic-element loading for bandwidth enhancement of loop antennas. The loop antenna used for study has a 3D-meander radiator for dual-band operation and a compact volume of only $5 \times 8 \times 60$ mm^3 [14], which can generate four resonant modes. To increase the bandwidth for the upper band, three additional resonant modes are generated by using three parasitic elements placed carefully on the substrate. This does not require any addition space. Thus the antenna altogether has seven resonant modes which can double the bandwidth of the upper band from 1.8–2.8 GHz (1 GHz, 43%) to 1.65–3.6 GHz (1.95 GHz, 74%) to support the DCS1800, PCS1900, UMTS2100, LTE2300, LTE 2500, and LTE 3500 systems. The enhanced bandwidth of the upper band is larger than that in [13, 14] by four times and two times, respectively. In terms of size, the proposed loop antenna has the size same as the one with $5 \times 8 \times 60 = 2{,}400$ mm^3 in [14] and smaller than the one with the size of $5 \times 13 \times 50 = 3{,}250$ mm^3 [13]. It is a dual band. The bandwidth of the lower band is 0.82–0.98 GHz (0.16 GHz, 17.8%) which can cover the GSM850 and GSM900 systems (requiring 0.824–0.96 GHz), same as the designs in [13, 14]. However, unlike the designs in [13, 14], the proposed loop antenna requires no matching circuit for the lower band, which can cut down the cost in the Bill of Material.

The preliminary study on the same design was reported by the authors in [17] which only illustrated the idea using computer simulation. However, in this paper, the proposed loop antenna with exactly the same design in [17] is prototyped. The antenna measurement equipment, the Satimo StarLab system [18], is used to measure the prototyped antenna. The operation of the antenna is analysed using current distribution. To study the antenna in the more practical scenarios, a phone case is made using 3D printing. The antenna placed inside the phone case on a phantom hand/head is measured in the 'data mode' and 'talk mode', respectively, as defined by the Cellular Telephone Industries Association (CTIA). The measured efficiency is subsequently used to estimate the total-radiated powers (TRPs) which are compared with the strictest over-the-air (OTA) testing requirement of Vodafone. Thus, the completed design of the loop antenna is described and studied in much more details, which was not done in previous literatures [1–17].

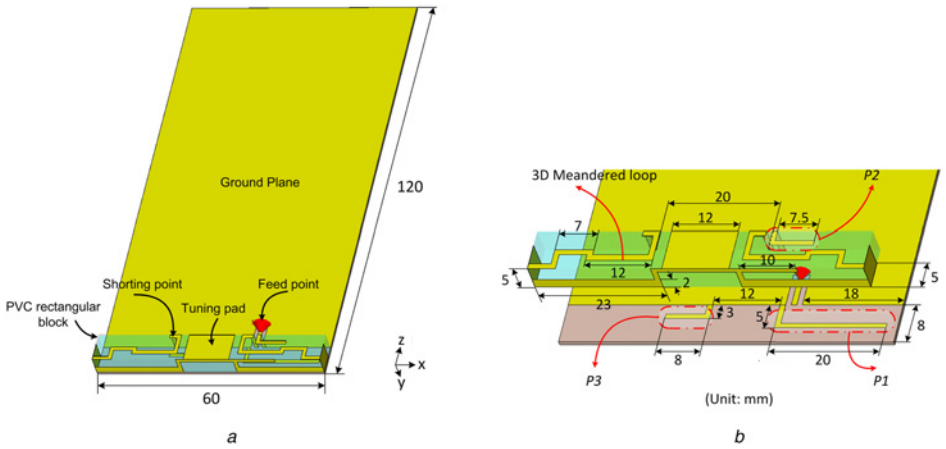

Fig. 1 *Geometry of loop antenna*

a 3D view on PCB
b Enlarged view of radiator

2 Proposed antenna

The proposed loop antenna is used for mobile-phones applications in the WWAN/LTE bands, with the geometry shown in Fig. 1*a*. The antenna is mounted in the lower side of the system printed-circuit board (PCB) having a standard dimension of 120×60 mm^2 for smartphones. An area of 8×60 mm^2 is made available for accommodation of the antenna. The antenna radiator mainly is a 3D-meandered loop. To increase the resonant modes, three parasitic elements are added, with detailed dimensions shown in Fig. 1*b*. *P*1 and *P*2 are placed close to the feed point in order to couple more energy for radiation. *P*3 is placed between the feed point and the shorting pin for more radiation, as it was shown in [14] that a strong current is following there from the feed point to the shorting pin. The 3D-meandered loop has width of 1 mm and a total length of 158 mm, equivalent to a length of about $\lambda/2$ (where λ is the guided wavelength) at 0.9 GHz, to generate three traditional resonant modes, the $\lambda/2$, 1.0λ and 1.5λ modes at 0.9, 1.86 and 2.12 GHz, respectively. The feed point and shorting point is separated at 20 mm to generate the 2.0λ mode, at 2.63 GHz [14, 15]. Thus, the 3D-meandered loop can generate four resonant modes. The $\lambda/2$ mode forms a lower band and the 1.0λ, 1.5λ and 2.0λ modes together form an upper band. A tuning pad with the size of 8×12 mm^2, as shown in Fig. 1*a*, is used to improve matching in the 1.0λ and 1.5λ modes [10, 11] and hence widen the bandwidth in the upper band. To maintain a rectangular shape, the loop radiator is mounted on the surface of a rectangular block made of polyvinyl chloride (PVC) with the dimension of $5 \times 8 \times 60$ mm^3, as indicated in Fig. 1*a*.

To improve the bandwidth of the upper band, three parasitic elements are used. They are denoted as parasitic elements *P*1, *P*2, and *P*3 in Fig. 1*b*. *P*1 and *P*3 are on the substrate under a block made of PVC, while *P*2 has a 3D folded element placed on the surface of the PVC block. Thus *P*1, *P*2 and *P*3 do not occupy any additional space. The lengths of *P*1, *P*2 and *P*3 are 25, 16 and 11 mm, respectively, which are equivalent to about $\lambda/4$ at 1.7, 3.25, and 3.55 GHz. These resonant frequencies are selected to maximise the bandwidth of the upper band. Computer simulation is used to design and study the antenna a Rogers substrate RO4350B with size 120×60 mm^2, thickness 0.8 mm, relative permittivity 3.48 and loss tangent 0.0037. The rectangular PVC block has $\varepsilon_r = 2.73$ and $\tan\delta = 0.01$. For measurement, the proposed antenna is prototyped, as shown in Fig. 2, and fed using a 50-Ω coaxial cable.

3 Antenna analysis

Computer simulation using the EM simulation tool CST is used to study the effects of the parasitic elements on the operation bandwidth of the antenna. Fig. 3 shows the simulated S_{11} of the antenna using only the meandered 3D-loop radiator, with only *P*1,

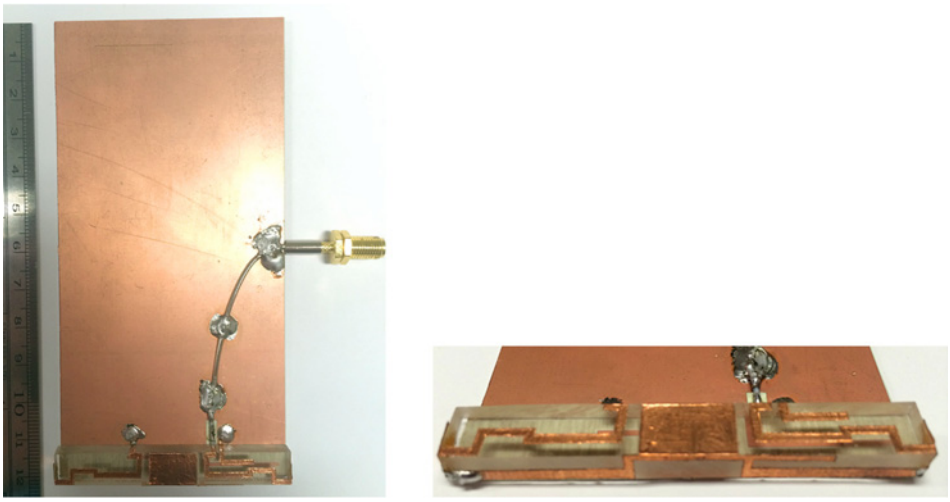

Fig. 2 *Prototyped antenna*

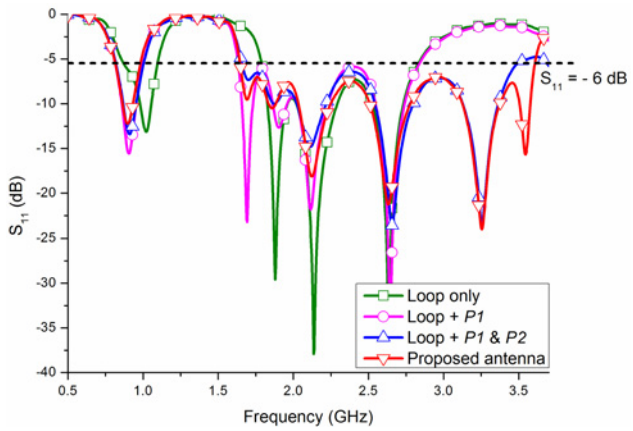

Fig. 3 *Simulated S_{11} of antenna with and without parasitic elements*

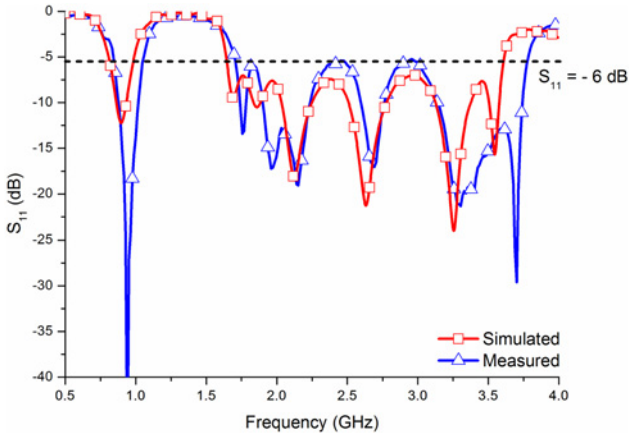

Fig. 5 *Simulated and measured S_{11} of proposed antenna*

with only *P*1 and *P*2, and with *P*1, *P*2 and *P*3. The result in Fig. 3 shows that the loop radiator itself generates four resonant modes, the λ/2, 1.0λ, 1.5λ and 2.0λ modes. The λ/2-mode at 0.9 GHz forms a low-frequency band and the 1λ, 1.5λ and 2.0λ modes at 1.86, 2.12 and 2.63 GHz, respectively, together form an upper-frequency band. With *P*1 added, Fig. 3 shows that a resonant mode is generated at 1.7 GHz in the upper band. The λ/2-mode only slightly shifts to a lower frequency and the resonant frequencies in the other modes remain almost unchanged. The upper band increases from 1.8–2.8 GHz (1 GHz, 43.5%) to 1.64–2.83 GHz (1.19 GHz, 53.2%). With *P*1 and *P*2 added, two resonant modes at 1.7 and 3.25 GHz are generated in the upper band. The bandwidth of the upper band further increases to 1.64–3.45 GHz (1.81 GHz, 70.6%). With all three parasitic elements added, the resonant modes at 1.7, 3.25, and 3.55 GHz increase the bandwidth of the upper band to 1.65–3.6 GHz (1.95 GHz, 74.3%), nearly doubling the bandwidth with only the loop radiator. The bandwidth of the lower band is 0.82–0.98 GHz (0.16 GHz,

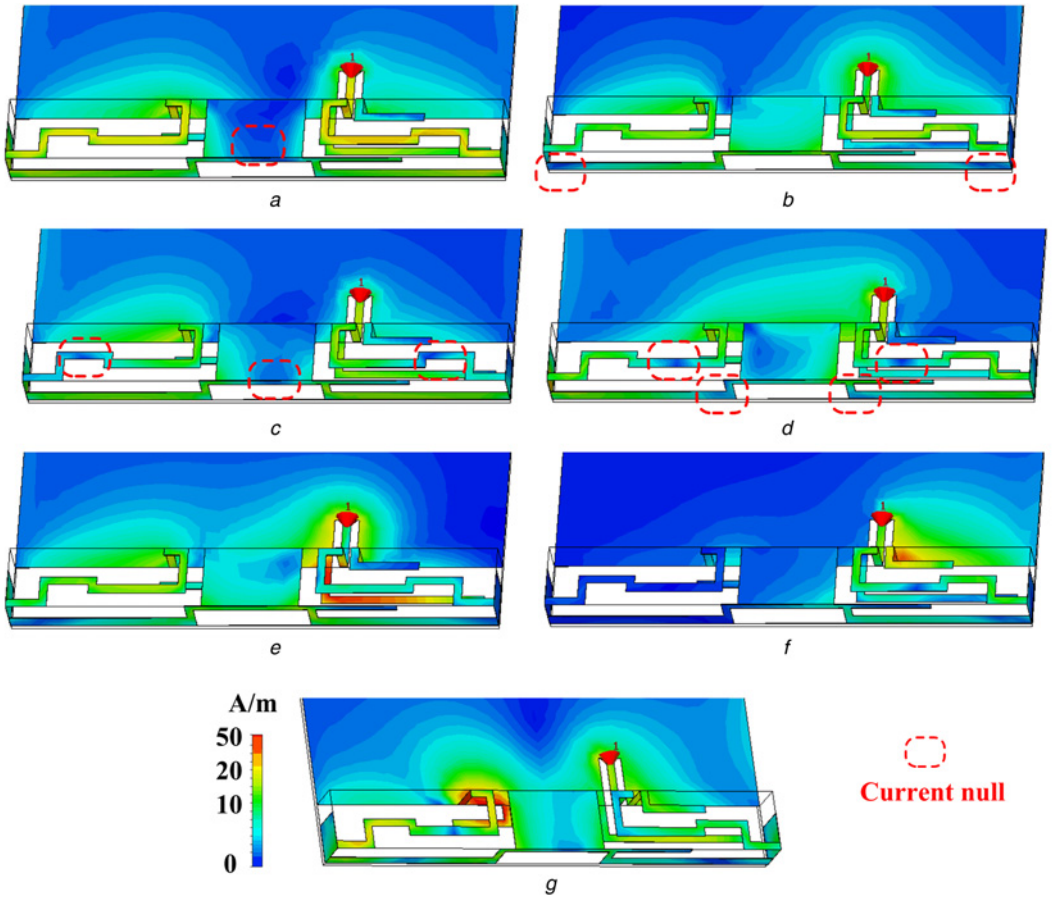

Fig. 4 *Surface current distributions at resonances*

a 0.9 GHz
b 1.86 GHz
c 2.12 GHz
d 2.63 GHz
e 1.7 GHz
f 3.25 GHz
g 3.55 GHz

IET Microw. Antennas Propag., 2017, Vol. 11, Iss. 2, pp. 240–246

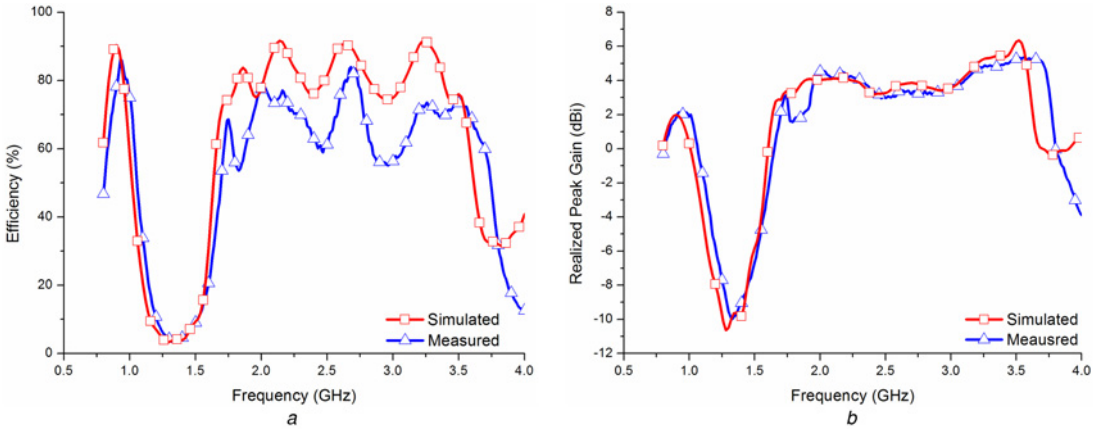

Fig. 6 *Simulated and measured radiation performance of proposed antenna*

a Efficiencies
b Gains

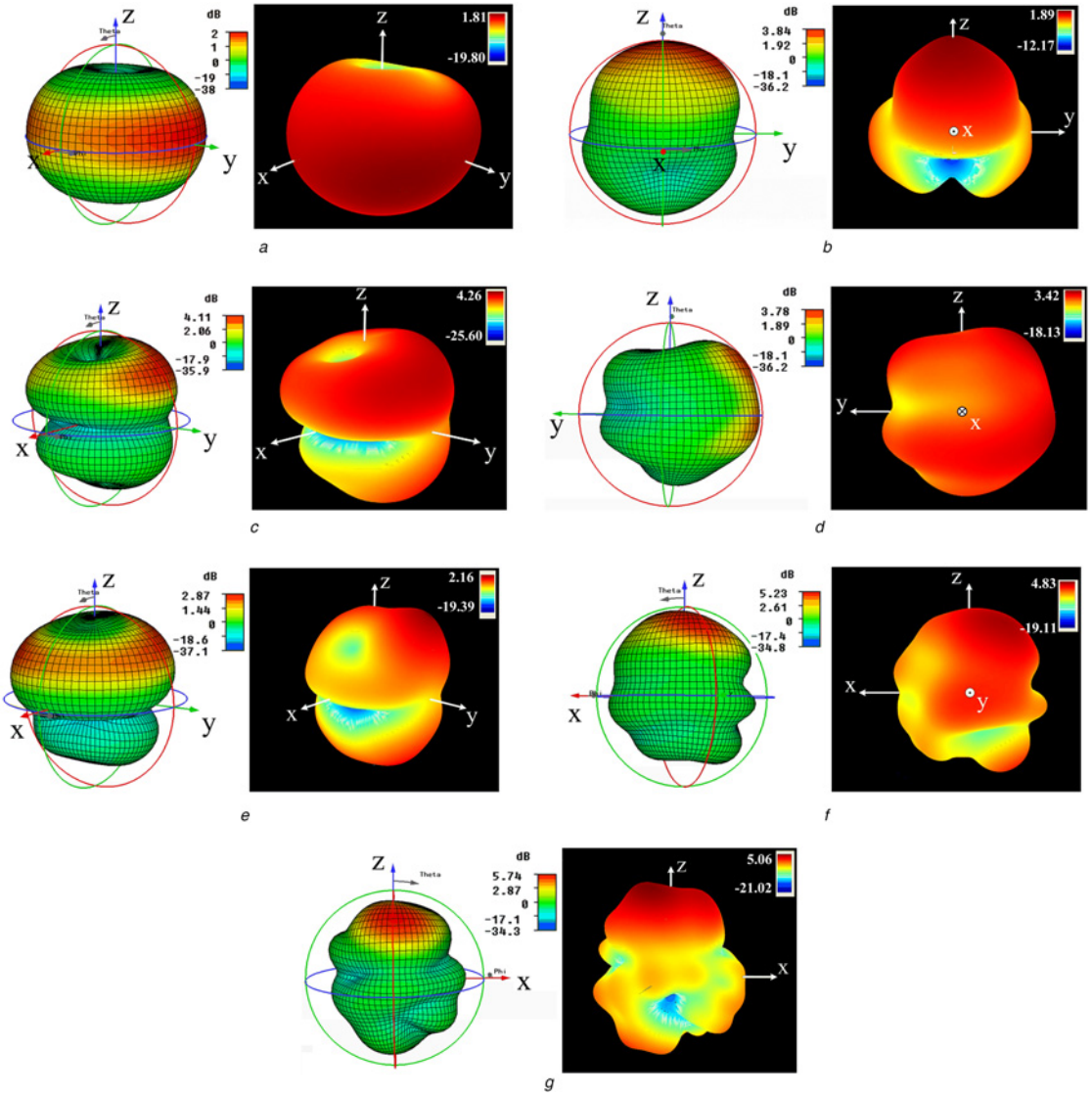

Fig. 7 *Simulated and measured 3D-radiation patterns at resonances*

a 0.9 GHz (sim) and 0.94 GHz (mea)
b 1.86 GHz (sim) and 1.96 GHz (mea)
c 2.12 GHz (sim) and 2.15 GHz (mea)
d 2.63 GHz (sim) and 2.7 GHz (mea)
e 1.7 GHz (sim) and 1.76 GHz (mea)
f 3.25 GHz (sim) and 3.28 GHz (mea)
g 3.55 GHz (sim) and 3.7 GHz (mea)

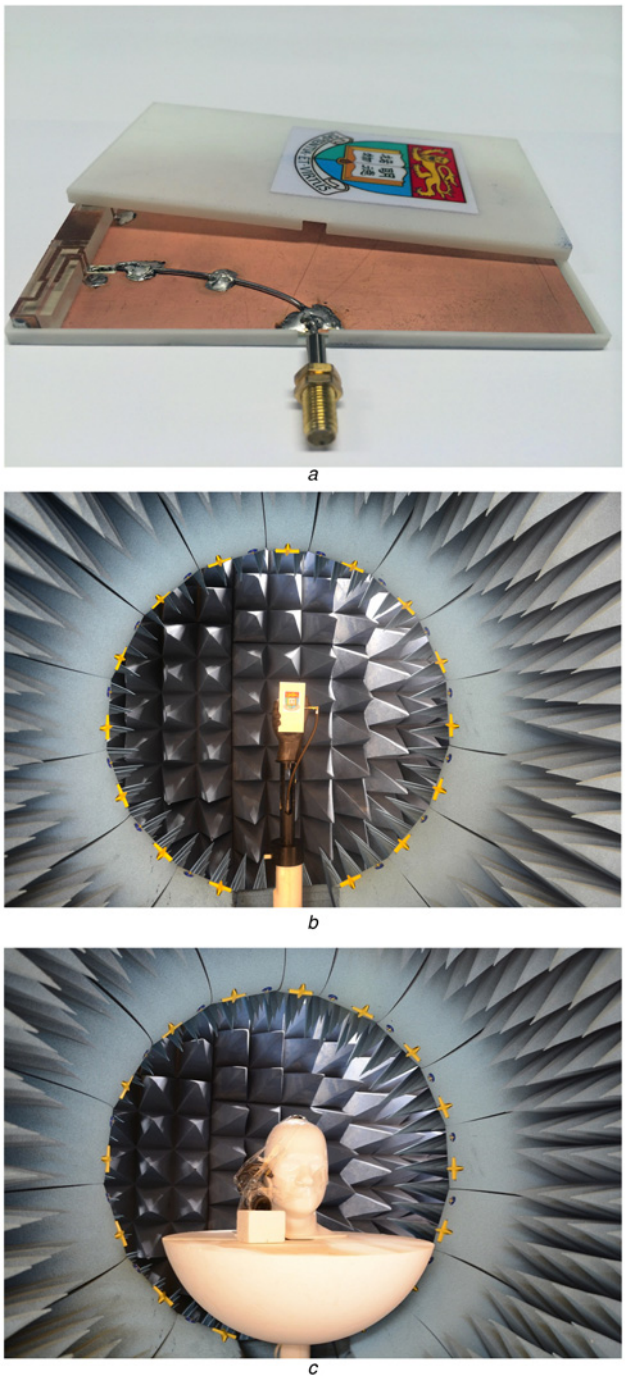

Fig. 8 *Antenna measurement in different scenarios*

a With phone case
b Data mode
c Talk mode

17.8%), larger than the required bandwidth 0.824–0.96 GHz for the GSM850 and GSM900 systems. Here no matching circuit is needed, which is an advantage over the designs in [13, 14].

Current distribution is used to further study the resonant modes of the antenna. Fig. 4 shows the simulated current distributions on the antenna radiator at different resonant modes. It can be seen in Figs. 4*a–d* that there are 1, 2, 3 and 4 current nulls on the loop radiator at 0.9, 1.86, 2.12, and 2.63 GHz, respectively, corresponding to the λ/2, 1.0λ, 1.5λ and 2.0λ resonant modes [14]. At the frequencies of 1.7, 3.25 and 3.55 GHz, parasitic elements #1, #2, and #3 have the strongest current densities as shown in Figs. 4*e–g*, respectively. Thus these parasitic elements are generating the corresponding resonant modes.

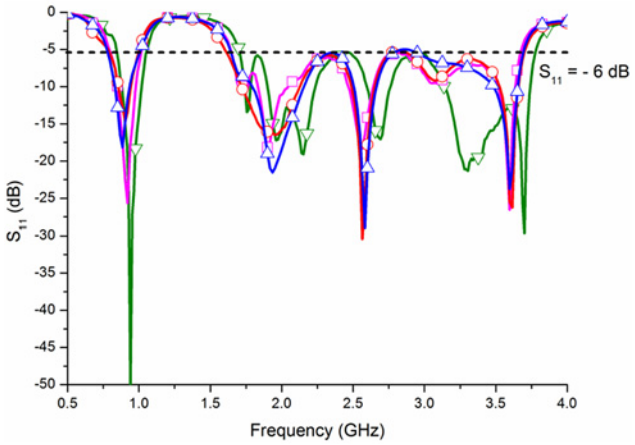

Fig. 9 *Measured S_{11} of antenna in different scenarios. (–∇– free space w/o housing; –□–free space with housing; –O–data mode; –Δ–talk mode)*

4 Results and discussion

The prototyped antenna of Fig. 3 has been measured. The results of S_{11} showed in Fig. 5 indicate a good agreement between simulation and measurement. The simulated result slightly differs from the measured result, mainly due to fabrication and measurement tolerances and the feeding cable effects [19, 20]. It can be seen that the antenna generates seven resonant modes which forms a dual band. The measured lower band is 0.83–1.03 GHz (0.2 GHz, 21.5%) and upper band is 1.7–3.78 GHz (2.08 GHz, 75.9%), which can support GSM850, GSM900, DCS1800 and PCS1900 in the 2G-standards, UMTS2100 in the 3G-standards, and LTE 2300, LTE 2500, and LTE3500 in the 4G and 5G standards. Note that $S_{11} \leq -6$ dB is used here to define the bandwidth, which is normally used in industry [21–24].

The simulated and measured efficiencies are shown in Fig. 6*a* and the simulated and measured peak gains are shown in Fig. 6*b*. The simulated and measured results have good agreements. The discrepancies are mainly due to fabrication and measurement tolerances and the feeding cable effects [19, 20]. The measured efficiency ranges from 60–86% in the low-frequency band and 55–83% in the high-frequency band, as indicated in Fig. 6*a*. The measured peak gain is about 0.6–2.1 dBi in the low-frequency band and 1.6–5.3 dBi in the high-frequency band, as indicated in Fig. 6*b*.

The results in 3D-radiation patterns are shown in Fig. 7. Note that the simulated resonant frequencies of the antenna are 0.9, 1.86, 2.12

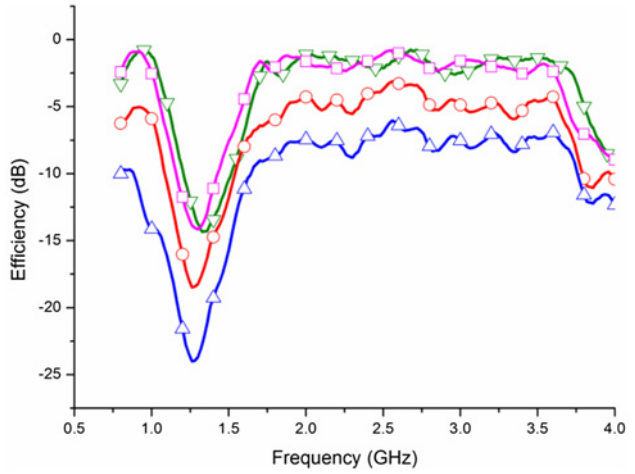

Fig. 10 *Measured efficiencies of antenna in different scenarios. (–∇– free space w/o housing; –□–free space with housing; –O–data mode; –Δ–talk mode)*

IET Microw. Antennas Propag., 2017, Vol. 11, Iss. 2, pp. 240–246

Table 1 Calculated TRP of antenna (NB: Vodafone V2.5 has no specified TRP for data mode)

	P_{cond}	GSM850 33	GSM900 33	DCS1800 30	PCS1900 30	UMTS2100 24	LTE2300 23	LTE2500 23	LTE3500 23
free space	efficiency	−1.37	−0.91	−1.94	−1.2	−1.3	−1.9	−0.81	−2.36
	TRP	31.63	32.09	28.06	28.8	22.7	21.1	22.19	20.64
	Vodafone TRP	25.5	27	24	22.5	18	N/A	N/A	N/A
talk mode	efficiency	−9.7	−10.5	−8.97	−7.7	−7.6	−8.53	−6.2	−7.29
	TRP	23.3	22.5	21.03	22.3	16.4	14.47	16.8	15.71
	Vodafone TRP	17.5	19	19	17.5	14	N/A	N/A	N/A
data mode	efficiency	−5.84	−5	−6.27	−4.89	−4.6	−5.28	−3.21	−4.63
	TRP	27.16	28	23.73	25.11	19.4	17.72	19.79	18.37

and 2.63 GHz for the loop and 1.7, 3.25 and 3.55 GHz for the parasitic elements, while the measured resonances are 0.940, 1.960, 2.150 and 2.70 GHz for the loop and 1.76, 3.28 and 3.7 GHz for the parasitic elements. It can be seen that the simulated and measured results all agree very well. In the 0.5-λ mode, Fig. 7*a* shows donut shapes. In the 1λ and 1.5λ modes, Figs. 7*b* and *c* show double donut shapes with slightly directional in the upper hemisphere (at the +*z*-direction). In the 2-λ, Fig. 7*d* shows patterns with mixture of single- and double-donut shapes. At about 1.7 GHz, the patterns as shown in Fig. 7*e* are generated by parasitic element #1 and also have double-donut shapes. At the higher frequencies of about 3.2 and 3.6 GHz, the patterns are shown in Figs. 7*f* and *g* and generated by parasitic elements #2 and #3, respectively. They are rather irregular, but also slightly pointing at the +*z*-direction. These are typical patterns for PIFAs and monopoles used in mobile phones [21–24].

5 Performances in more practical conditions

In practice, the antenna will be installed inside a phone case. When used, the mobile phone will be placed closely to the user's head or the hand. In such cases, the performance will be severely affected. In fact, the CTIA has defined these two cases as the mobile in the 'talk mode' and 'data mode' with specified test methods for performance assessment [25].

Thus here we also study the performances of the antenna inside a phone case, in the data mode and in the talk mode. To study the effects of phone case on the antenna, a phone case with a dimension of $61 \times 121 \times 6.8$ mm^3 and a thickness of 0.5 mm is fabricated using 3D printing. The antenna is fixed inside as shown in Fig. 8*a*. The printing material for the phone case is acrylonitrile butadiene styrene with $\varepsilon_r = 2.30$ and tan $\delta = 0.028$. Since phone case with antenna inside is a device which has a width of 61 mm (between 56–72 mm), according to the specifications of CTIA V3.4 [25], the PDA grip method as illustrated in Fig. 8*b* should be used to measure the performance in the data mode. In our measurement, the phantom hand used is Model IXB-053 from IndexSAR [26], which is made of carbon fibre, carbon powder, and silicone rubber with the permittivity (ε_r) and conductivity (σ) similar to those of a human hand in the frequency band from 300 MHz to 6 GHz, i.e. $\varepsilon_r = 20$ to 33 and $\sigma = 0.36$ to 3.5. For measurement in the talk mode, according to CTIA V.3.4 [25], the device should be held by a phantom hand and placed closely to the ear of the phantom head as illustrated in Fig. 8*c*. The phantom head used in our measurement is provided by SATIMO [18] and filled with liquid equivalent material having the permittivity (ϵ_r) and conductivity (σ) similar to those of a human head in the frequency band from 300 MHz to 6 GHz, i.e. $\epsilon_r = 35$ to 45 and $\sigma = 0.8$ to 5.5.

The measured S_{11} of the antenna inside the phone case in free space, in the data mode and in the talk mode are shown in Fig. 9. For comparison, the measured S_{11} without the phone case is also shown in the same figure. It can be seen that the phone case only slightly shifts the resonances to lower frequencies, and the phantom hand (in the data mode) and phantom head (in the talk mode) further slightly shift the resonances to lower frequencies. As far as bandwidth is concerned, the worst case is in the talk mode where the antenna has the bandwidths of 0.79–1 GHz and 1.66–3.69 GHz in the low- and upper bands, respectively. Thus the lower band can still cover the GSM850 standard and the GSM900 standard (requiring a bandwidth of 0.824–0.96 GHz) and the higher band can cover the DCS1800, PCS1900, UMTS2100, LTE2300, LTE2500, LTE3500 systems (requiring the bandwidth of 1.71–3.6 GHz).

The measured efficiencies of the antenna with phone case in free space, and in the data mode and talk mode are shown in Fig. 10. The efficiency is expressed in dB which will be used to compute the TRP later. It can be seen that the phone case does not reduce the antenna efficiency much, but the phantom hand and phantom head significantly degrade the efficiency. In the lower band and with using the phone case, the peak efficiency drops from −0.88 dB at 0.92 GHz in free space to −5.03 dB at 0.92 GHz in the data mode, and then further to −9.86 dB at 0.86 GHz in the talk mode. At 2.7 GHz (the centre frequency in the higher band), the efficiency drops from −1.49 dB in free space to −3.4 dB in the data mode, and then to −6.64 dB in the talk mode.

Total-isotropic sensitivity (TIS) and TRP in OTA testing are usually used to assess the performances of mobile phones in the mobile phone industry. Many cellular-network providers such as Vodafone and AT&T require their mobile phones to have the certain minimum values of TRP and TIS. TIS depends on the antenna and the sensitivity of the receiver, and so cannot be measured using the antenna alone. However, TRP is a measure of how much power is radiated by an antenna and can be estimated using the following empirical formula [22]:

$$\mathrm{TRP(dB}m) = P_{\mathrm{cond}}(\mathrm{dB}m) + \mathrm{Efficiency(dB)} \quad (1)$$

which is based on the assumption that matching between the power amplifier output and the antenna of the mobile is achieved and grounding and shielding of the active devices of the mobile phone are good. In (1), P_{cond} is the conductive power from the output of the power amplifier. According to 3GPP [27], the value of P_{cond} used is different in different mobile standards. For example, P_{cond} is 33 dBm for the GSM850/GSM900 systems, 30 dBm for the DCS1800/PCS1900 systems, 24 dBm for the UMTS2100 (WCDMA Band I), and 23 dBm for the LTE2300/LTE2500 /LTE3500 systems. With the use of (1), the measured efficiency of Fig. 10 and the specified P_{cond} in 3GPP [27], the TRP of the antenna in free space, in the data mode and in talk mode for different mobile standards are calculated and compared with the required values of Vodafone [28] in Table 1. It should be noted that among different cellular-network operators, Vodafone has the strictest specifications [28]. For simplicity of Table 1, only the middle channel in each frequency band is used, i.e. ch189 at 836.4 MHz for GSM850, ch37 at 897.4 MHz for GSM900, ch698 at 1747.4 MHz for DCS1800, ch661at 1880MHz for PCS1900, ch9750 at 1950MHz for WCDMA Band I, ch27710 at 2310 MHz for LTE2300, ch21100 at 2535 MHz for LTE2500, and ch25000 at 3450 MHz for LTE3500. It can be seen in Table 1 that the antenna meets the Vodafone's TRP requirement in all mobile standards covered in the lower and upper bands.

6 Conclusions

A loop antenna with compact volume for mobile phones applications has been designed. The loop radiator can generate four resonant modes. Three parasitic elements are placed closely to the loop to generate three more resonant modes. These seven resonances form a dual band, a lower and an upper band. The loop antenna designed has been fabricated for measurement. The loop antenna has a lower band of 0.82–0.98 GHz covering GSM850 and GSM900 in the 2G-standard and an upper band of 1.65–3.6 GHz covering DCS1800 and PCS1900 in the 2G standard, UMTS2100 in the 3G standard and LTE2300, LTE2500 and LTE3500 in the 4G and 5G standard. The effects of phone case, phantom hand and phantom head on the performances of the antenna have been studied. The measured efficiency has been used to estimate the TRP in different mobile standards. Results have shown that the antenna can satisfy the strictest TRP requirement of Vodafone.

7 References

1 Abutarboush, H.F., Nilavalan, R., Peter, T., *et al.*: 'Multiband inverted-F antenna with independent bands for small and slim cellular mobile handsets', *IEEE Trans. Antennas Propag.*, 2011, **59**, (7), pp. 2636–2645

2 Chang, C.H., Wong, K.L.: 'Printed l/8-PIFA for penta-band WWAN operation in the mobile phone', *IEEE Trans. Antennas Propag.*, 2009, **57**, (5), pp. 1373–1381

3 Wong, K.L., Tu, M.F., Wu, C.Y., *et al.*: 'Small-size coupled-fed printed PIFA for internal eight-band LTE/GSM/UMTS mobile phone antenna', *Microw. Opt. Technol. Lett.*, 2010, **52**, pp. 2123–2128

4 Ban, Y.L., Chen, J.H., Li, L.W., *et al.*: 'Small-size printed coupled-fed antenna for eight-band LTE/GSM/ UMTS wireless wide area network operation in an internal mobile handset', *IET Microw. Antennas Propag.*, 2013, **7**, (6), pp. 399–407

5 Deng, C.J., Li, Y., Zhang, Z.J., *et al.*: 'Planar printed multi-resonant antenna for octa-band WWAN/LTE mobile handset', *IEEE Antennas Wirel. Propag. Lett.*, 2015, **14**, pp. 1734–1737

6 Kang, D.G., Sung, Y.: 'Coupled-fed planar printed shorted monopole antenna for LTE/WWAN mobile handset applications', *IET Microw. Antennas Propag.*, 2012, **6**, (9), pp. 1007–1016

7 Li, Y., Zhang, Z.J., Zheng, J.F., *et al.*: 'A compact hepta-band loop-inverted F reconfigurable antenna for mobile phone', *IEEE Trans. Antennas Propag.*, 2012, **60**, pp. 389–392

8 Li, Y., Zhang, Z.J., Zheng, J.F., *et al.*: 'Compact heptaband reconfigurable loop antenna for mobile handset', *IEEE Antenna Wirel. Propag. Lett.*, 2011, **10**, pp. 1162–1165

9 Ban, Y.L., Chen, Z.X., Chen, Z., *et al.*: 'Reconfigurable narrow-frame antenna for heptaband WWAN/LTE smartphone applications', *IEEE Antenna Wirel. Propag. Lett.*, 2014, **13**, pp. 1365–1368

10 Chi, Y.W., Wong, K.L.: 'Compact multiband folded loop chip antenna for small-size mobile phone', *IEEE Trans. Antennas Propag.*, 2008, **56**, pp. 3797–3803

11 Wong, K.L., Huang, C.H.: 'Printed loop antenna with a perpendicular feed for penta-band mobile phone application', *IEEE Trans. Antennas Propag.*, 2008, **56**, pp. 2138–2141

12 Ishimiya, K., Chiu, C.Y., Takada, J.: 'Multiband loop handset antenna with less ground clearance', *IEEE Antennas Wirel. Propag. Lett.*, 2013, **12**, pp. 1444–1447

13 Zheng, M., Wang, H.Y., Hao, Y.: 'Internal hexa-band folded monopole/dipole/loop antenna with four resonances for mobile device', *IEEE Trans. Antennas Propag.*, 2012, **60**, (6), pp. 2880–2885

14 Wu, D., Cheung, S.W., Yuk, T.I.: 'A compact and low-profile loop antenna with multiband operation for ultra-thin smartphones', *IEEE Trans. Antennas Propag.*, 2015, **63**, (6), pp. 2745–2750

15 Ban, Y.L., Li, C., Sim, C.Y.D., *et al.*: '4G/5G multiple antennas for future multi-mode smartphone applications', *IEEE Access*, 2016, **4**, pp. 2981–2988

16 Wong, K.L., Tsai, C.Y.: 'Small-size stacked inverted-F antenna with two hybrid shorting strips for LTE/WWAN tablet device', *IEEE Trans. Antennas Propag.*, 2014, **62**, pp. 3962–3969

17 Wu, D., Cheung, S.W., Yuk, T.I.: 'A compact loop antenna with seven resonant modes for smartphones'. 2015 IEEE-APS Topical Conf. on Antennas and Propagation in Wireless Communications (APWC), Turin, Italy, 2015, pp. 355–358

18 'SATIMO'. Available at http://www.satimo.com, accessed 20 Feb 2016

19 Liu, L., Cheung, S.W., Weng, Y.F., *et al.*: 'Cable effects on measuring small planar UWB monopole antennas' in Matin, M. (Ed.): 'Ultra Wideband-Current Status and Future Trends' (Intech, 2012), pp. 273–294

20 Chen, Z.N., Yang, N., Guo, Y.X., *et al.*: 'An investigation into measurement of handset antennas', *IEEE Trans. Instrum. Meas.*, 2005, **54**, pp. 1100–1110

21 Wong, K.L.: 'Planar antennas for wireless communications' (Wiley, New York, 2003)

22 Zhang, Z.J.: 'Antenna Design for Mobile Devices' (John Wiley & Sons, Singapore, 2011)

23 Anguera, J., Andújar, A., Huynh, M.C., *et al.*: 'Advances in antenna technology for wireless handheld devices', *Int. J. Antennas Propag.*, 2013, Article ID 8383643

24 Rowell, C., Lam, E.Y.: 'Mobile-phone antenna design', *IEEE Antennas Propag. Mag.*, 2012, **54**, pp. 14–34

25 'CTIA Test Plan for Mobile Station Over-the-Air Performance', Rev. 3.4, December 2014

26 'IndexSAR Online'. Available at http://indexsar.com, accessed 20 Feb 2016

27 'The 3rd Generation Partnership Project (3GPP)'. Available at http://www.3gpp.org/, accessed 20 February 2016

28 'Vodafone Specification for Terminals on Over the Air RF Performance', Version 2.5, 2012